Transforming Growth Factor-β_1 Specifically Induce Proteins Involved in the Myofibroblast Contractile Apparatus*

Johan Malmström‡, Henrik Lindberg‡, Claes Lindberg‡, Charlotte Bratt‡§, Elisabet Wieslander¶, Eva-Lena Delander¶, Bengt Särnstrand‖, Jorge S. Burns, Peter Mose-Larsen**, Stephen Fey**, and György Marko-Varga‡ ‡‡**

Transforming growth factor-β_1 (TGF-β_1) induces α-smooth muscle actin (α-SMA) and collagen synthesis in fibroblast both *in vivo* and *in vitro* and plays a significant role in tissue repair and the development of fibrosis. During these processes the fibroblasts differentiate into activated fibroblasts (so called myofibroblasts), characterized by increased α-SMA expression. Because TGF-β_1 is considered the main inducer of the myofibroblast phenotype and cytoskeletal changes accompany this differentiation, the main objective of this investigation was to study how TGF-β_1 alters protein expression of cytoskeletal-associated proteins. Metabolic labeling of cell cultures by [^{35}S]methionine, followed by protein separation on two-dimensional gel electrophoresis, displayed ~2500 proteins in the p*I* interval of 3–10. Treatment of TGF-β_1 led to specific spot pattern changes that were identified by mass spectrometry and represent specific induction of several members of the contractile apparatus such as calgizzarin, cofilin, and profilin. These proteins have not previously been shown to be regulated by TGF-β_1, and the functional role of these proteins is to participate in the depolymerization and stabilization of the microfilaments. These results show that TGF-β_1 induces not only α-SMA but a whole set of actin-associated proteins that may contribute to the increased contractile properties of the myofibroblast. These proteins accompany the induced expression of α-SMA and may participate in the formation of stress fibers, cell contractility, and cell spreading characterizing the myofibroblasts phenotype. ***Molecular & Cellular Proteomics 3:466–477, 2004.***

A characteristic feature of asthma is the remodeling of the subepithelial compartment of the bronchial airway wall, sometimes referred to as subepithelial fibrosis. The remodeling involves increased production of collagen I, III, and V, fibronectin, and proteoglycans (1). One of the mechanisms for the excess production of extracellular matrix molecules has been proposed to be due to an increase in the number of differentiated bronchial myofibroblasts (2). The myofibroblasts play a central role in wound healing (3–7) and appear to be involved in the formation and repair of the extracellular matrix (8–10; for review see 6, 7, 11). The myofibroblasts are characterized by antibody reactions against components in the intracellular microfilaments such as α-smooth muscle actin (α-SMA)[1] and members of the intermediary filament like vimentin, desmin, and laminin (12, 13). In an activated state, the myofibroblasts also stain positive for muscle heavy chain myosin (also known as tropomyosin) (14, 15). Another distinguishing feature of the myofibroblasts is their ability to secrete large amounts of matrix molecules, such as collagens and proteoglycans, compared with the fibroblasts (16, 17), which are proteins found in increased levels in fibrotic tissue (18–23). The transformation of fibroblasts to myofibroblasts can be caused by different exogenous stimuli, where the main factor is considered to be transforming growth factor β_1 (TGF-β_1) (24–27). Both *in vivo* and *in vitro*, TGF-β_1 alters the fibroblast phenotype to one that resembles the features of myofibroblasts, including increased expression of α-SMA (21, 26–33), collagen, fibronectin, and proteoglycan synthesis (24, 27, 28, 31, 34). TGF-β_1 is also one of the main growth factors in tissue repair and in the development of fibrosis (19, 27, 34, 35). TGF-β_1 signals via two serine/threonine kinase receptors TRI and TRII, and the SMAD-signaling pathway constitutes the main signal transduction route downstream of the these receptors. In fibroblasts, TGF- β_1 induces rearrangements of the actin filament system and rapid formation of lamellipodia (36). This response was shown to be independent of the

From the ‡Department of Molecular Sciences, AstraZeneca R&D Lund, SE-221 87 Lund, Sweden; ¶Department of Bioscience, AstraZeneca R&D Lund, SE-221 87 Lund, Sweden; ‖Department of Clinical Development, AstraZeneca R&D Lund, SE-221 87 Lund, Sweden; and **The Center for Proteome Analysis in Life Science, University of Southern Denmark, Forskerparken 10/B, Odense, Denmark

Received, October 9, 2003, and in revised form, January 28, 2004
Published, MCP Papers in Press, February 6, 2004, DOI 10.1074/mcp.M300108-MCP200

[1] The abbreviations used are: α-SMA, alpha smooth muscle actin; TGF-β, transforming growth factor β; TNF-α, tumor necrosis factor α; PPM-IOD, parts-per million integrated optical density; MALDI-TOF, matrix-assisted laser desorption/ionization time-of-flight; ESI-MS, electrospray ionization mass spectrometry; 2-D PAGE, two-dimensional PAGE; 2-DE, two-dimensional electrophoresis; SMAD, mothers against decapentaplegic homolog; HFL-1, human fetal lung fibroblasts; FCS, fetal calf serum; LSM, low serum medium; hsp, heat shock protein.

SMAD-signaling pathway; instead, it required the activity of the Rho GTPases Cdc42 and RhoA (36). Long-term stimulation with TGF- β_1 resulted in an assembly of stress fibers; this response however required both signaling via Cdc42, RhoA, and SMAD proteins (36). Activation of RhoA by TGF-β_1 is also important for formation of stress fibers in the epithelial to mesenchymal transdifferentiation (37). Fibroblasts positive for α-SMA have a different phenotype than fibroblasts negative for α-SMA (38). The increased level of α-SMA found in myofibroblast is potentially important for the contractile features of these cells under repair and fibrotic conditions. Therefore, an increased knowledge of the molecular mechanism behind the induction of α-SMA would be of interest. Previous findings from our group show that by stimulating HFL-1 cells with TGF-β_1 several tropomyosin isoforms were up-regulated (39). The main aim of this study was to provide a more detailed quantitative study of changes in actin-associated proteins induced by TGF-β_1 using [^{35}S]methionine metabolic-labeling human fibroblasts and two-dimensional gel electrophoresis (2-DE).

EXPERIMENTAL PROCEDURES

Materials

The chemicals used were purchased from Merck (Stockholm, Sweden). The recombinant human cytokines tumor necrosis factor α (TNF-α) (R&D Systems, Minneapolis, MN) and TGF-β (R&D Systems) were diluted from stock solutions according to the manufacturer's recommendations.

Cell Culture

The human primary fetal lung cell line (HFL-1) was purchased from American Tissue Culture Collection (Manassas, VA). The HFL-1 cells were grown in T-75 flasks (Costar; Myriadindustries, San Diego, CA) with minimum Eagle's medium (MEM) (M-4655; Sigma, Stockholm, Sweden) supplemented with 10% fetal calf serum (FCS) (Life Technologies, Paisley, United Kingdom) and 2 mM L-glutamine (Life Technologies) at 37 °C in 5% CO_2 until confluence. All experiments were performed below passage 18. Low serum medium (LSM) containing 0.4% FCS was used for labeling and stimulation experiments. For the immunohistological staining, the HFL-1 cells were grown in 12-well plates and treated with TGF-β_1. After 48 h, the cells were detached with trypsin, washed with phosphate-buffered saline, adhered to adhesion slides (Bio-Rad, Hercules, CA), fixed in ethanol, and air dried and stored in −80 °C until staining. Staining was performed with anti-human α-SMA mouse monoclonal antibody (Dako, Copenhagen, Denmark) or isotype for control. Visualization was made with a Vectastain ABC kit. The α-SMA positive cells were quantified by counting 400 cells per sample, and the experiments were repeated four times.

Metabolic Labeling of Cells with [^{35}S]Methionine

For Analytical Gels—The protocol for metabolic labeling has been described previously (40). Briefly, the cells were plated in a 1:2 dilution series in 96-well plates (1 well = 0.32 cm^2) starting with 2.5 × 10^6 cells/ml and 100 μl/well. After 24 h, wells with confluent cells were selected and the medium in these wells was changed to LSM. For comparison, cells were plated in a 96-well plate at a concentration of 12,500 cells/ml and were allowed to grown to confluence for a week,

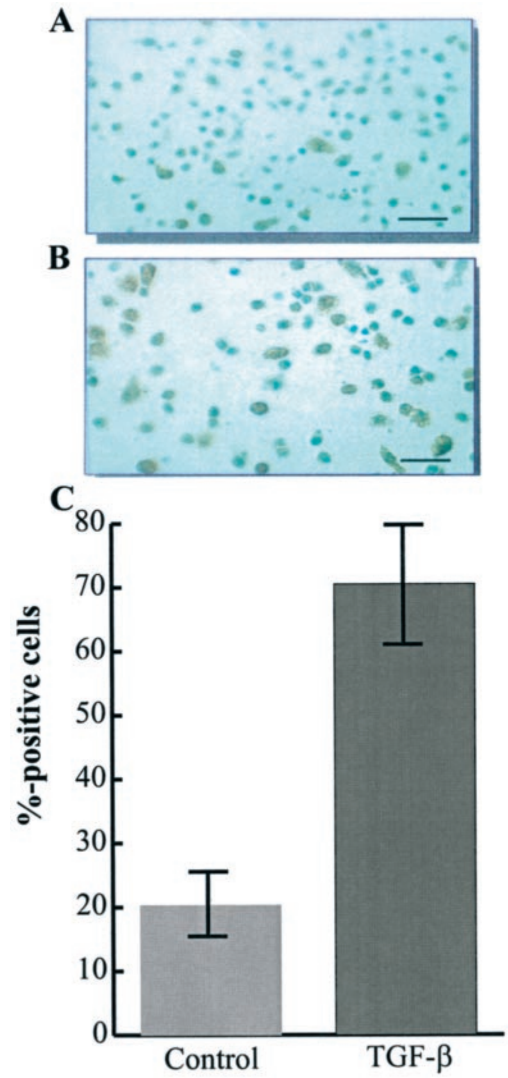

FIG. 1. **TGF-β_1 induces expression of α-SMA in fibroblasts.** HFL-1 cells were treated with TGF-β_1 for 48 h and the amount of α-SMA was determined by immunohistochemistry. *A*, cell culture after isotype control. *B*, antibody to α-SMA. *C*, the percentage of stained cells with or without TGF-β_1 treatment (n = 4 experiments).

followed by switching to LSM. After an additional 24 h, the cells were washed once with Hanks' buffered saline and once with labeling medium. Labeling medium consisted of MEM without methionine (M-3911; Sigma) supplemented with 0.4% FCS, 2 mM L-glutamine, and 0.5 μg/ml cold methionine (M-7520; Sigma). The [^{35}S]methionine (SJ235; Amersham Pharmacia Biotech, Uppsala, Sweden) was lyophilized in a speedvac overnight before use to remove the stabilizing agent β-mercaptoethanol and redissolved in labeling medium to a final concentration of 1000 μCi/ml. After washing, 100 μl of medium containing [^{35}S]methionine was added to the wells and incubated for various lengths of time so that the cells were exposed to radiolabel for an equivalent period of 20 h in all experiments. Thus, the control cells (t = 0) were radiolabeled for 20 h in 110 μl of medium. For 30 min of TGF-β stimulation, the cells were prelabeled with medium containing [^{35}S]methionine for 19.5 h and then 10 ng/ml TGF-β_1 was added (t = 30 min). For 6 h of TGF-β stimulation, the cells were prelabeled for 14 h and then 10 ng/ml TGF-β_1 was added (t = 6 h). At harvest, the

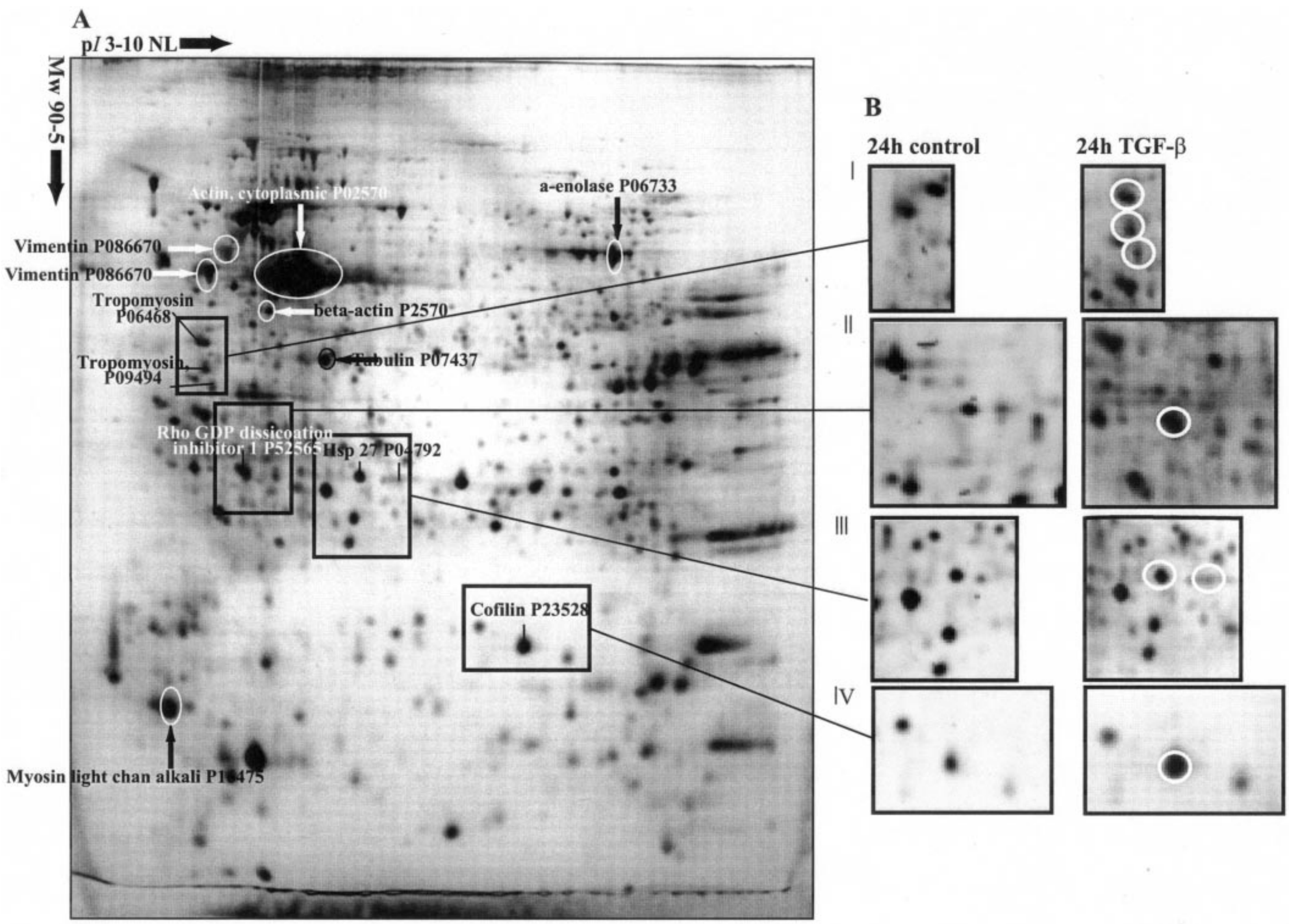

FIG. 2. **Differential protein expression pattern of human fibroblast stimulated with TGF-β for 24 h.** Differential protein expression pattern of human fibroblast stimulated with TGF-β_1 for 24 h. After cell solubilization, the protein homogenate was separated by 2-DE according to "Experimental Procedures." *A*, TGF-β_1-stimulated cell culture separated by Immobiline dry strips with a pI interval of 3–10NL. Only cytoskeletal-associated proteins are marked on the gel image. *B*, segments with regulated proteins compared with a control-treated cell culture. *I*, Tropomyosin isoforms; *II*, Rho-GDP dissociation inhibitor; *III*, hsp27; and *IV*, cofilin.

cells were washed with Hanks' buffer and then lysed in 8 M urea and 2% 3-[(3-cholamidopropyl)dimethylammonio]-1-propanesulfonic acid (CHAPS). The incorporation of [^{35}S]methionine in the samples was measured by scintillation counting.

For Preparative Gels—the cells were plated at 2.5 × 10^5 cells (in 2 ml) in six-well plates and grown to confluence. The medium was changed to LSM and the procedure described for the analytical gels was followed, except that only 100 μCi [^{35}S]methionine per well was used. The cells were lysed in 500 μl 8 M urea and 2% CHAPS. The sample was precipitated with ice-cold acetone to avoid excess of salt and lipids present in the cell preparations. The sample was mixed with acetone to a final concentration of 80% acetone and incubated on ice for 40 min and then centrifuged 20,000 rpm in a Sorvall centrifuge.

Two-dimensional Gel Electrophoresis

Immobiline Dry strips (180 mm, pH 3–10 NL) were rehydrated in 350 μl of the solubilized cell lysate supplemented with 10 mM dithiothreitol (DTT) and 0.5% immobilized pH gradient 3–10 buffer (Amersham Pharmacia Biotech). The isoelectrofocusing step was performed at 20 °C in an IPGphor™ (Amersham Pharmacia Biotech) and run according to the following schedule: (1) 30 V for 10 h, (2) 500 V for 1 h, (3) 1000 V for 1 h, and (4) 8000 V until ~65,000 Vh was reached. The strips were equilibrated for 10 min in a solution containing 65 mM DTT, 6 M urea, 30% (w/v) glycerol, 2% (w/v) SDS, and 50 mM Tris-HCl, pH 8.8. A second equilibration step was also carried out for 10 min in the same solution except for DTT, which was replaced by 259 mM iodoacetamide. The strips were soaked in electrophoresis buffer (24 mM Tris base, 0.2 M glycine, and 0.1% SDS) just before the second-dimensional gel electrophoresis. The strips were applied on 14% homogeneous Duracryl slabgel. The strips were overlaid with a solution of 1% agarose in electrophoresis buffer (kept at 60 °C). Electrophoresis was carried out in a Hoefer™ DALT gel apparatus (Amersham Pharmacia Biotech) at 20 °C and constant 100 V for 18 h.

After electrophoresis, the gels were dried using a gel dryer (model 583; Bio-Rad). Small pieces of filter paper were dipped in diluted isotope solution and dried in air and used as markers. The markers were glued on the dried gel before placing it in the imager cassette. After 10 days, the [^{35}S]methionine-labeled proteins were visualized by

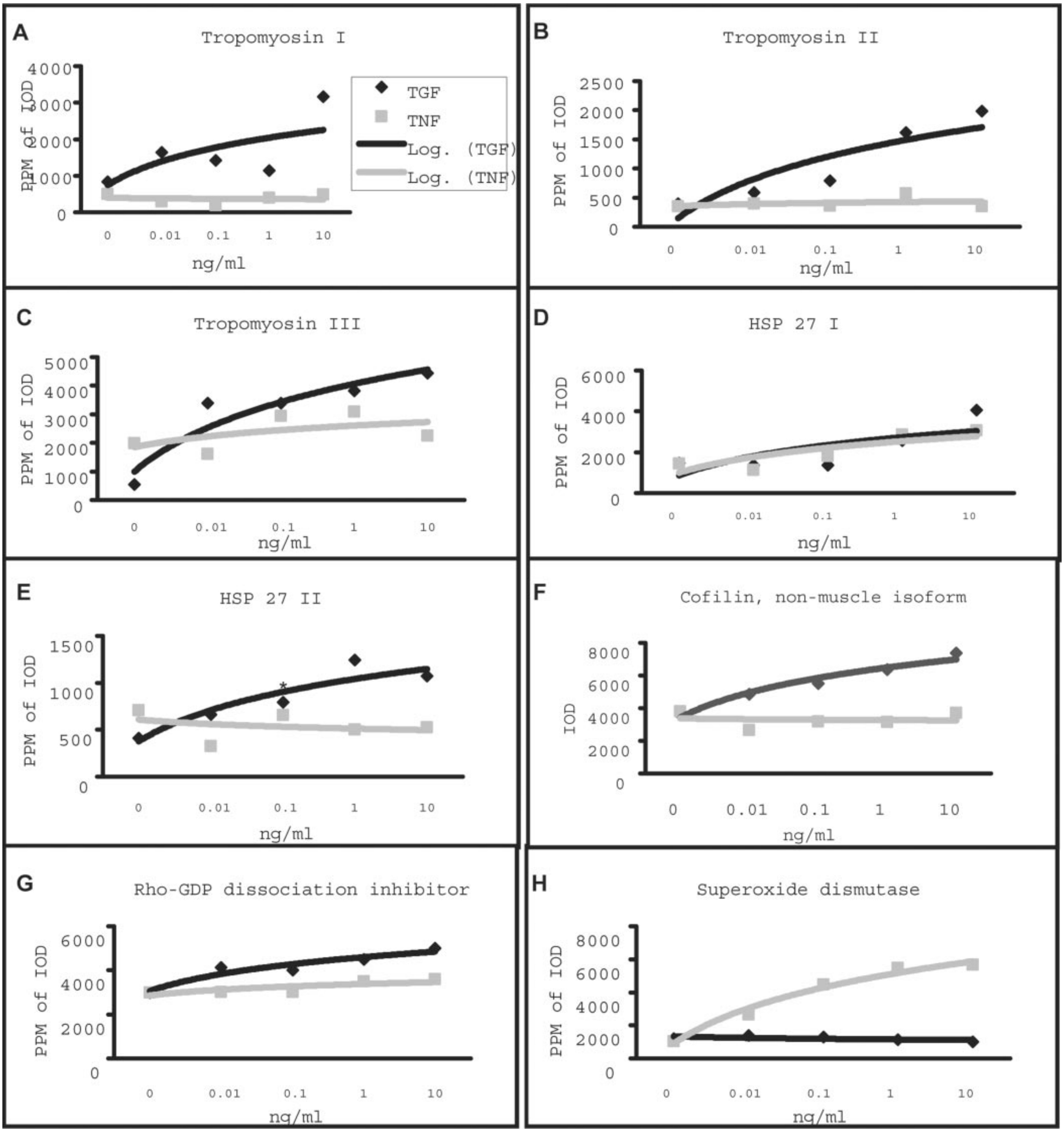

FIG. 3. **Specific dose-dependent TGF-β_1-induced protein expression compared with TNF-α.** Regulated proteins were plotted in a dose-dependent manner corresponding to cytokine concentrations of 0.01, 0.1, 1, and 10 ng/ml. The proteins shown are significantly induced after cytokine stimulation and associated with actin or stress fiber formation. *A*, tropomyosin I; *B*, tropomyosin II; *C*, tropomyosin III; *D*, hsp27 I; *E*, hsp27 II; *F*, cofilin; *G*, Rho-GDP dissociation inhibitor; and *H*, superoxide dismutase.

using an imager (STORM 860; Molecular Dynamics (now part of Amersham Biosciences), Sunnyvale, CA).

Gel Staining—In some cases, the gels were silver stained as described previously (41) or stained with SyproRuby (Molecular Probes, Eugene, OR) according to the manufacturer's recommendations.

Computer-assisted Analysis of Protein Expression in 2-D Gels

Spot analysis was performed using the PDQuest (version 6.1.0) two-dimensional gel analysis system (Bio-Rad). Every spot on the gel is given an integrated optical density (IOD) value that was compared

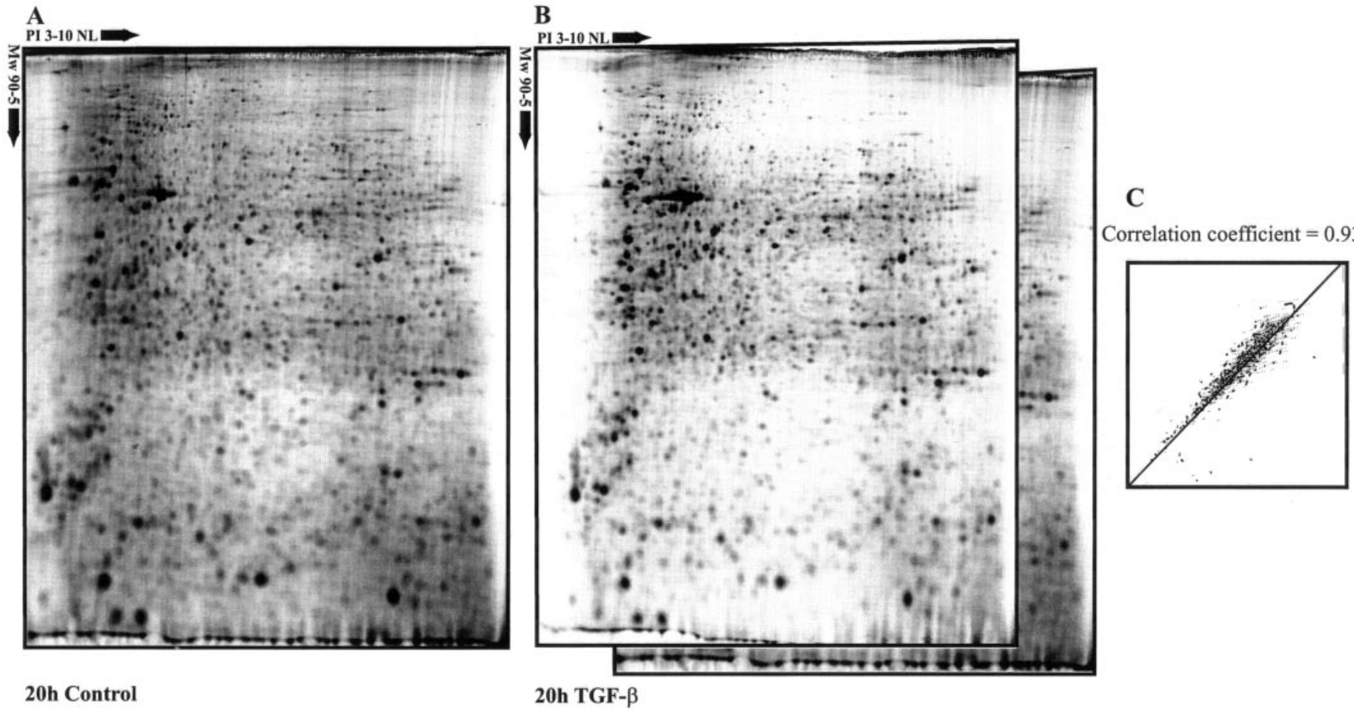

FIG. 4. **Evaluation of the developed [^{35}S]methionine protocol.** The sample was prepared according to the "Experimental Procedures": 3–10NL isoelectricfocusing strips were used to separate protein in the first dimension and 14% polyacrylamide gels in the second dimension. *A*, a representative analytical gel from one control sample; and *B*, TGF-β_1-treated sample showing ~3000 spots. *C*, the correlation coefficient between two replicates of the TGF-β_1-treated sample was 0.93.

with the total from all valid spots. Thus, each spot has a relative intensity expressed as parts per million (PPM) of the total IOD of all valid spots. Each spot on the gel from stimulated samples was compared with the corresponding spot on the gel with the control-treated sample.

Identification by Mass Spectrometry

Tryptic Digestion—After image analysis, the gel spots were excised from the gel and transferred to separate Eppendorf vials. The gel pieces were washed with ammonium bicarbonate buffer (50 mM) followed by acetonitrile extraction three times. Reduction and alkylation of the excised spots was followed by tryptic digestion overnight using 10 μl cold trypsin solution 10 ng/μl (Boehringer, Mannheim, Germany).

Mass Spectrometry—The matrix-assisted laser desorption/ionization time-of-flight (MALDI-TOF) instrument was a DE-PRO Voyager mass spectrometer (Applied Biosystems, Framingham, MA). The instrument, equipped with a delayed extraction ion source, utilized a nitrogen laser at 337 nm and was operated in reflector mode at an accelerating voltage of 20 kV. The sample probes were made of polished stainless steel. Alpha-cyano-4-hydroxycinnamic acid (α-CHCA) was used as matrix employing the dried droplet technique or elution of peptides purified on reversed-phase microcolumns (42). Tandem mass spectrometry was performed using a nano-electrospray ionization (ESI) spray on a quadrupole TOF mass spectrometer (Micromass, Manchester, United Kingdom). The sample was loaded in precoated borosilicate nano-electrospray needles (MDS Protana, Odense, Denmark; now Protana Engineering A/S). The source temperature was set to 40 °C. A potential of 1 kV was applied to the nano-electrospray needles, and 50 V was applied as the cone voltage. Argon was used as a collision gas at a pressure of 6–7 $\times$ 10^{-5} mbar, and the collision energy was 20–30 V. Product ions were analyzed using an orthogonal TOF analyzer. Data processing was performed with Mass Lynx Window NT PC system.

Statistics

Mean ± SE were calculated. Student's *t* test was used to evaluate the differences of the means between groups.

RESULTS

TGF-β_1 Stimulation Induced α-SMA Expression in Human Fibroblasts

TGF-β_1 induced a 4- to 6-fold increase (from 20 to 70%) of detectable α-SMA protein determined by immunocytochemical staining after 48 h as shown in Fig. 1, indicative of myofibroblast differentiation as previously has been described (12, 13). The TGF-β_1 response was similar throughout passages 15–18, so these passages were used for further experiments.

Protein Separation by 2-DE of Cell Cultures Treated with TGF-β_1 or TNF-α

In the next set of experiments, the stimulated HFL-1 cell lysate was separated by 2-DE to study changes in the protein expression pattern after stimulation with TGF-β_1 or TNF-α. The concentrations used were 0.01, 0.1, 1, and 10 ng/ml for 24 h. Proteins of interest were identified by MALDI-TOF MS and/or ESI-MS/MS. A representative expression map is shown in Fig. 2. After 24 h, but not after 6 h, TGF-β_1 induces several proteins associated with the cytoskeleton, such as three isoforms of tropomyosin, two isoforms of heat shock protein (hsp) 27, Rho-GDP dissociation inhibitor, and cofilin, whereas myosin light chain, vimentin, tubulin, and β-actin were not induced (data not shown). TNF-α induced the expression of superoxide dismutase, as has previously been described (43) (Fig. 3*H*). The up-regulation induced by TGF-β_1 was dose-dependent and specific compared with TNF-α (see Fig. 3). The induced expression of the tropomyosin isoforms ranged from 5- to 8-fold compared with control ($p < 0.05$–0.01) shown in Fig. 3, *A*–*C*, the two hsp27 isoforms were up-regulated 2.7-fold shown in Fig. 3, *D* and *E* ($p < 0.01$–0.001), cofilin 2-fold ($p < 0.05$) shown in Fig. 3*F*, and Rho-GDP dissociation inhibitor 1.8-fold ($p < 0.01$) shown in Fig. 3*G*.

[^{35}S]Methionine Labeling of HFL-1 Cells Prior to TGF-β_1 Stimulation

The number of regulated spots observed after silver staining was limited. We therefore modified a methodology for [^{35}S]methionine metabolic labeling, which is a more sensitive compared with both silver and fluorescent staining techniques (44, 45). Silver staining reveals proteins present in the sample, whereas metabolic labeling focuses on newly synthesized proteins and can thus more effectively reveal cellular responses to a stimulus. The developed protocol increased the number of high-quality protein spots observed in the master gels from 800 to 2400 (Fig. 4). The reproducibility of this protocol was better than that of silver staining when using 100 μg total amount of protein. The correlation coefficient of 0.9 within replicate sets was considered satisfactory ($n = 24$ gels) (46) (see Fig. 4). An additional gain by using [^{35}S]methionine labeling as compared with silver staining is the much wider linear dynamic range of about five orders of magnitude compared with the 40-fold linear dynamic range before saturation for silver staining. The differences in the appearance between the gels stained with silver and the [^{35}S]methionine metabolic labeling protocol largely reflects the latter method focused on newly synthesized proteins. Additional differences may account for the fact that the two staining methods rely on different amino acids.

Induced Expression of Actin-associated Proteins upon Exposure to TGF-β_1

The increased number of visualized spots was used to monitor the effect of TGF-β_1 on HFL-1 cells over a 20-h time period. TGF-β stimulation was performed by incubating the HFL-1 cells with [^{35}S]methionine for a total of 20 h, including TGF-β_1 stimulation for 30 min, 6 h, and 20 h. From the triplicate 2-D gels from every time point it can be seen that the total number of expressed proteins over time was rather constant while the number of proteins regulated by TGF-β_1 increased with time from ~50 to ~100. The procedure, including cell culture, stimulation, harvest, 2-D PAGE, and image

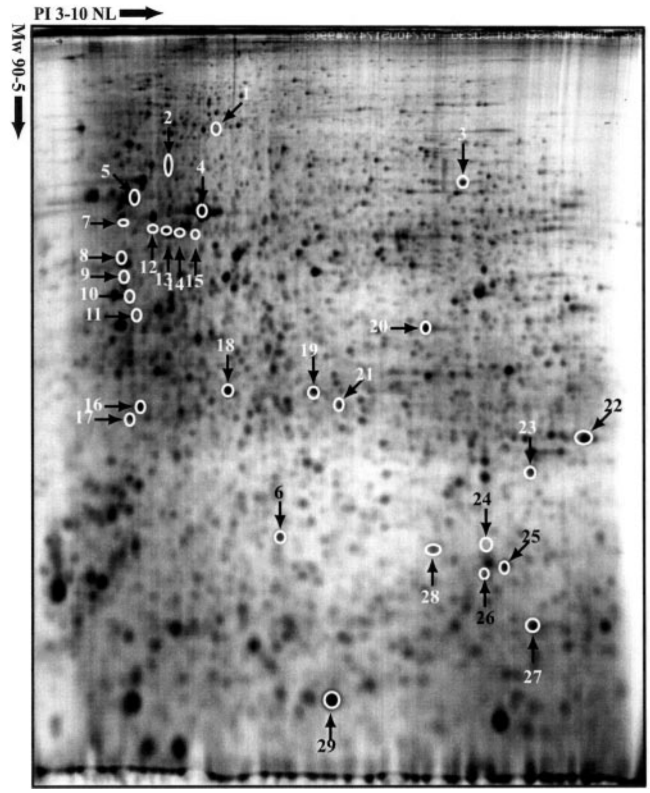

FIG. 5. **Protein expression profiling after TGF-β_1 stimulation using [^{35}S]methionine labeling and 2-DE.** HFL-1 cells were labeled with [^{35}S]methionine and stimulated with TGF-β_1 for 30 min, 6 h, and 20 h. The proteins were separated by 2-D SDS-PAGE, and the proteins were visualized by autoradiography. Proteins were identified with MALDI-TOF MS or ESI MS/MS. The gels shown are from a master gel representing gels from a control-treated cell culture. Marked spots represent identified proteins and correlates to the numbers shown in Table I and Fig. 6.

analysis, was repeated five times. The combined output from three different strategies was used to select statistically regulated spots: 1) lower level match set where all gels at a certain time point (*e.g.* 24 h of stimulation) were included into a single match set and the statistical variation was calculated, 2) higher level match set, and 3) export of the raw data from PDQuest into a relational database in which regulated spots could be selected. Eighteen of the regulated spots were identified from the preparative gels and are shown in Fig. 5 plus 11 identified landmark proteins. The protein names are shown in Table I, and the expression pattern of the regulated proteins are shown in Fig. 6. The proteins were not induced at 30 min nor 6 h, but after 20 h of TGF-β_1 stimulation. Most were known to be associated with the cytoskeleton, either by binding to actin or by involvement in contractile features of the cells (Fig. 6). Proteins that have previously been shown to be induced by TGF-β are marked with a star in Table I. The proteins found to be differentially expressed in this study were SPARC precursor (osteonectin), 2.3-fold ($p < 0.03$); TGF-β-

TABLE I
Identified [^{35}S]methionine-labeled proteins

No. on gel[a]	Protein name[b]	A.K.A.[c]	Acc. No.[d]	M_r[e] (kDa)
1	T-complex protein 1, ϵ subunit		P48643	60.0
2	Vimentin		P08670	53.5
3	α Enolase		P06733	47.3
4	Actin, cytoplasmic 1		P02570	42.0
5	Vimentin		P08670	53.5
6	Stathmin		P16949	17.1
7	SPARC precursor*	Osteonectin	P09486	35.4
8	Tropomyosin, fibroblast, and epithelial type*		P06468	32.8
9	Tropomyosin, fibroblast isoform TM3*		P09494	32.7
10	Tropomyosin, cytoskeletal type*		P12324	32.8
11	Tropomyosin α chain, skeletal muscle*		P09493	32.7
12	Calponin, acidic isoform*		Q15417	36.5
13	Calponin, acidic isoform*		Q15417	36.5
14	Calponin, acidic isoform*		Q15417	36.5
15	Calponin, acidic isoform*		Q15417	36.5
16	CYR61 protein	Caldesmon	Q05682	93.2
17	TGF-β-induced protein*		Q15582	74.6
18	Heat shock 27 kD protein (hsp27)*		P04792	22.4
19	Heat shock 27 kD protein (hsp27)*		P04792	22.4
20	Annexin II (calpactin heavy chain)		P07355	38.4
21	Protein-L-isoaspartate-*O*-methyltransferase		P22061	24.5
22	Smooth muscle protein 22-α*	Transgelin	Q01995	22.5
23	SM22-α homolog*	Transgelin 2	P37802	22.5
24	DNA-binding protein		Q13403	19.3
25	Peptidyl-prolyl *cis-trans* isomerase A		P05092	18.1
26	Peptidyl-prolyl *cis-trans* isomerase A		P05092	18.1
27	Profilin		P07737	15.0
28	Cofilin		P23528	18.7
29	Calgizzarin		P31949	11.8

[a] The numbers correlate to the marked numbers on the master gel in Fig. 5.
[b] Proteins previously shown to be induced by TGF-β (see text for details).
[c] A.K.A., Also known as.
[d] Swissprot accession number.
[e] M_r, molecular mass.

induced protein, 2.8-fold ($p < 0.045$); four isoforms of tropomyosin, 1.5- to 11.1-fold ($p < 0.01$–0.05); CYR61 protein (caldesmon), 1.7-fold ($p < 0.03$); two isoforms of hsp27, 3- and 5-fold ($p < 0.05$–0.001); two isoforms of smooth muscle protein 22-α (transgelin 1 and 2), 1.8- and 3-fold ($p < 0.05$–0.01); profilin, 2.6-fold ($p < 0.001$); cofilin, 3-fold ($p < 0.01$); and calgrizzin, 1.6-fold ($p < 0.05$) (number of experiments $n = 3$). Identities are included in the reference image showing a protein number corresponding to the number in Table I (see Fig. 5).

In addition, it is also shown in the magnified spot trails in Fig. 7 how the expression of different isoforms of calponin is affected by TGF-β_1 stimulation (spots 12–15 in Fig. 5). Three of the calponin isoforms were significantly up-regulated by a factor of 4.6 ($p < 0.001$), 2.6 ($p < 0.01$), and 2.1 (0.05), whereas one was induced (1.7-fold) but not significantly. The sequence coverage of the three isoforms were 23, 42, 38, and 34%, respectively and are displayed in Fig. 7*B*. The type of post-translational modification cannot be determined from MS spectra alone and needs to be further investigated. Nonetheless, the spot pattern informs us that there is a relatively large shift in isoelectric point between the isoforms, which is the pattern normally associated with changes in phosphorylation.

DISCUSSION

TGF-β is considered one of the main inducers of the differentiation of fibroblasts into myofibroblasts (25). Because α-SMA is important for the phenotypic features and contractile properties of the myofibroblasts, we wished to extend our knowledge of cytoskeletal proteins accompanying this up-regulation. To provide a more comprehensive study of the protein changes upon TGF-β_1 stimulation of human lung fibroblasts, a 2-D gel proteomic approach was used comparing two methods of protein visualization and quantification. Significant up-regulation of a number of actin-associated and calcium-binding proteins was observed.

When using silver staining, a typical protein expression pattern consisted of 1000–1500 spots in each gel. Silver staining of two-dimensional gels in a pI interval of 3–10 does to some extent enable study of the regulation of proteins belonging to the contractile apparatus of the fibroblast. How-

# on Gel	Protein Name	Acc. Nr.	Ratio	p-value
	ECM			
7	SPARC precursor	P09486	2.3	0.0297
17	Transforming growth factor-beta induced protein	Q15582	2.8	0.0451
	Cytoskeletal			
6	Stathmin	P16949	0.6	0.0288
8	Tropomyosin, fibroblast and epithelial type	P06268	2.0	0.0178
9	Tropomyosin, cytoskeletal type	P12324	1.5	0.0538
10	Tropomyosin, fibroblast isoform TM3	P09494	6.1	0.0234
11	Tropomyosin alpha chain, skeletal muscle	P09493	11.3	0.0122
12	Calponin, acidic isoform	Q15417	4.6	0.0014
13	Calponin, acidic isoform	Q15417	2.6	0.0112
14	Calponin, acidic isoform	Q15417	1.7	0.1500
15	Calponin, acidic isoform	Q15417	2.2	0.0509
16	CYR61 protein	Q05682	1.7	0.0271
18	Heat shock 27 kD protein (HSP 27)	P04792	2.1	0.0128
19	Heat shock 27 kD protein (HSP 27)	P04792	2.9	0.0008
22	SM22-alpha homolog	P37802	1.9	0.0295
23	Smooth muscle protein 22-alpha	Q01995	3.0	0.0254
27	Profilin	P07737	2.6	0.0003
28	Cofilin	P23528	3.2	0.0045
29	Calgizzarin	P31949	1.6	0.0499

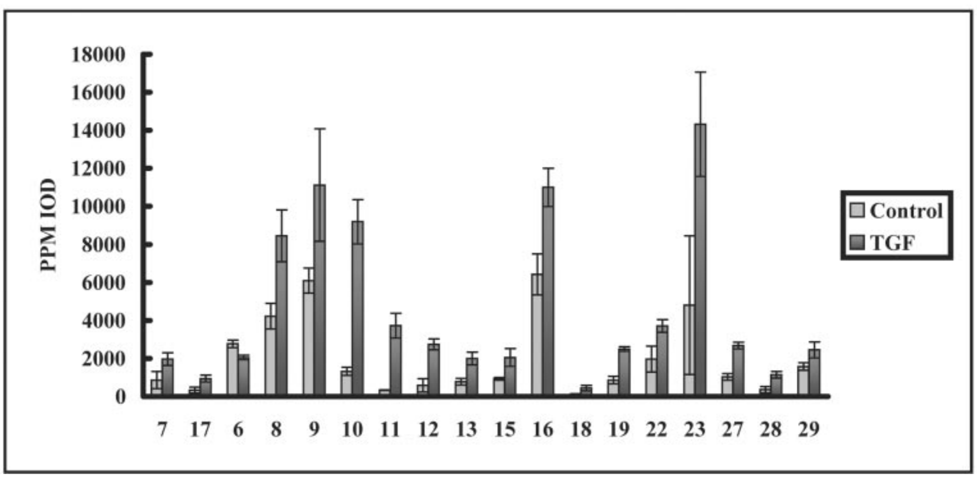

FIG. 6. **TGF-β_1 stimulation results in induced expression of several proteins that are either actin binding or calcium binding.** Statistical significantly induced proteins after 20 h of TGF-β_1 stimulation that have either actin-binding or calcium-binding properties. The protein numbers to the far left are shown on a gel on Fig. 5 and Table I. PPM-IOD is the optical density of the spots correlated to the total optical density for all spots present in the gel.

ever, by developing a protocol for metabolic labeling with [^{35}S]methionine there was a marked 3-fold improvement in the overall number of high-quality proteins spots detected on the master gels (from 800 to 2400). The major protein spots in a silver-stained gel were also found in the [^{35}S]methionine gels, and the overall pattern was similar. Nonetheless, the metabolic [^{35}S]methionine approach has the advantage of only displaying newly synthesized proteins. In addition, the linear dynamic range before saturation for silver-stained gels is about 40-fold, whereas use of radioisotope provides five orders of magnitude.

TGF-β_1 induced a strong expression of α-SMA in the majority of the HFL-1 cells. The functional role of the α-SMA regulation is to increase the contractility of the myofibroblast (47). The protein expression pattern induced by TGF-β_1 stimulation was compared with the pattern seen after TNF-α treatment to determine the specificity of the response. Even though some of the regulated proteins responded to both TGF-β_1 and TNF-α, like hsp27, most regulated proteins were cytokine specific. It is thus possible to obtain specific cytokine-driven protein regulation patterns in HFL-1 cells. In addition, when comparing the TGF-β_1 effects on Mv1Lu lung epithelial cells determined by 2-DE, the induced proteins were vastly different, indicating a cell-specific response to TGF-β_1 (48). In this study, the main effect of TGF-β_1 stimulation of human lung fibroblast was the induction of several proteins

A

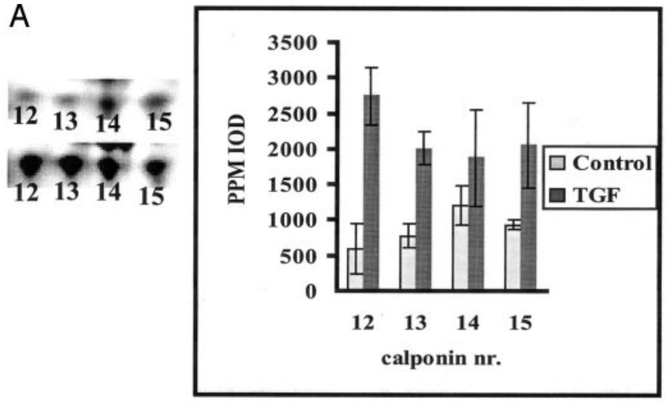

B

Mr (calc)	Start	End	Miss	Peptide	Mr (observed) spotnr. for Caloponin 12	13	14	15
750.367	151	156	1	RFDEGK	751.361	751.367	751.36	751.37
771.395	187	192	0	HLYDPK	772.384	772.383	772.38	-
780.367	227	232	0	DIYDQK	781.358	781.351	-	-
938.465	257	265	0	GM**S**VYGLGR*	939.47	939.475	939.473	939.476
954.457	257	265	0	GM**S**VYGLGR*	955.456	-	955.46	955.463
1106.562	7	17	0	GPSYGLSAEVK	1107.569	1107.56	1107.556	1107.56
1186.637	133	143	0	GFHTTIDIGVK	-	1187.636	1187.639	1187.637
1215.602	213	225	0	GASQAGMLAPGTR	1216.622	1216.618	1216.624	1216.623
1231.594	213	225	0	GASQAGMLAPGTR	1232.604	1232.597	1232.609	1232.606
1274.551	24	33	0	YDHQAEEDLR	-	1275.574	1275.575	1275.579
1372.586	173	185	0	CA**S**QAGM**T**AYGTR*	1373.613	1373.605	1373.612	1373.606
1388.578	173	185	0	CA**S**QAGM**T**AYGTR*	1389.602	1389.588	1389.597	1389.586
1402.727	159	172	0	AGQSVIGLQMG**T**NK*	1403.731	1403.72	1403.74	1403.717
1415.781	131	143	1	TKGFHTTIDIGVK	1416.749	-	-	-
2059.062	233	251	0	LTLQPVDNSTISLQMGTNK	-	2060.062	2060.1	2060.077
2283.09	193	212	0	MQTDKPFDQTTISLQMGTNK	-	2284.069	-	2284.058
2299.082	193	212	0	MQTDKPFDQTTISLQMGTNK	-	2300.098	-	-

*Peptides containing potential phosphorylation sites described previously (see text for details)

FIG. 7. **Zoom segment illustrating calponin isoforms regulated upon TGF-β_1 stimulation.** HFL-1 cells were stimulated with TGF-β for 20 h and the cell lysate was separated by 3–10NL strips and 14% homogenous gels. The proteins were visualized with [^{35}S]methionine. *A*, TGF-β_1 induces the expression of four calponin isoforms with similar molecular mass but with different pI, indicative of a post-translational modification. *B*, The four spots were identified as calponin with a sequence coverage of 23, 42, 38, and 34%, respectively. Peptides displayed matched to calponin in the database with a mass error of less than 50 ppm. The peptides sequences marked with a star contain previously described phosphorylation sites, all of which are found as unmodified in the four MS spectra.

responsible for an increase of stress fibers. Several of these proteins has previously been shown to be induced by TGF-β_1: SPARC precursor (osteonectin) (49), TGF-β-induced protein (50), tropomyosin (39), hsp27 (51), smooth muscle protein 22-α (transgelin 1 and 2) (52), and calponin (53). However, in addition we find that CYR61 protein (caldesmon), Rho-GDP dissociation inhibitor, profilin, cofilin, and calgizzarin are induced after 20 h of TGF-β_1 stimulation, thus showing that in parallel to the induction of α-SMA other actin-associated proteins are induced. Cofilin and profilin activates actin filament polymerization (54). Profilin catalyzes the exchange of ADP for ATP, returning subunits to the pool of ATP-actin bound to profilin, ready to elongate barbed ends of the actin filaments as they become available (55). Cofilin is required for the formation of barbed ends at the leading edge of the actin filaments (56, 57) and severs actin, thereby increasing the number of free barbed ends leading to enhanced Arp2/3 complex activation (58). In this study, we found that tropomyosin was also induced, which in contrast to cofilin and profilin, stabilizes the actin filaments and inhibits nucleation and branch formation of the Arp2/3 complex (59) and the cofilin-F-actin interaction *in vitro* (60–62). The mutual up-regulation of tropomyosin, profilin, and cofilin seems contradictory, but may be explained by a model proposed by DesMarais *et al.* (63). They found that, upon epidermal growth factor stimulation, all isoforms of tropomyosin were absent from the extreme dynamic leading edge compartment of lamellipodia, but rather co-localized deeper in the lamellipodia and in stress fibers, whereas cofilin was localized in the extreme leading edge of the lamellipodia. Thereby, the tropomyosin-free-actin filaments in the extreme leading edge just under the membrane can participate in actin branching and polymerization, whereas tropomyosin inhibits the branching and stabilizes the actin-filaments elsewhere in the cell (63).

Calponin, calgizzarin, smooth muscle protein 22-α (transgelin), and tropomyosin have previously been characterized as smooth muscle markers and are induced in smooth muscle differentiation (64). Additionally in some tissues, myofibroblasts stain positive for muscle heavy chain myosin or tropomyosin (old terminology), caldesmon, and desmin (6, 14, 15), perhaps explaining the contractile properties of the myofibroblast. Calponin is a thin filament-associated protein that has also been implicated in the modulation of the contractile apparatus in smooth muscle cells via its interaction with actin (65). The suggested role of calponin is mediated by inhibition of the actin-activated myosin Mg-ATPase (65). When calponin is phosphorylated either by PKC or Rho at Thr^{170}, Ser^{175}, Thr^{180}, and Thr^{259}, the binding of calponin to F-actin is inhibited (66). An up-regulation of the phosphorylated isoforms suggest increased contractile capability of the fibroblast. However, in this study, all of the potential phosphorylation sites were, within the matched peptides, indicating that these peptides are unmodified or that given sensitivity limits the spectra do not resolve this modification. An explanation can be that the peptides in fact are phosphorylated but not detected because they do not bind well to the micropurification columns used or the documented fact of ion suppression when detecting the phosphopeptides, which necessitates different MS strategies for their detection (67). Therefore additional experiments are required to determine the type of post-translational modification seen in this case. Calgizzarin is a calcium-binding protein (68) that has been found in developing skeletal muscles (69). Expression and subcellular localization of calgizzarin has been shown to be affected in aging (70) and immortalization of fibroblasts (71, 72). Thus, we find in this study that TGF-β_1 induced several proteins that are either actin- or calcium-binding proteins and whose function has been implicated in the formation of contractile stress fibers. Several of the proteins are also known smooth muscle cell markers, suggesting that TGF-β_1 induces a more contractile hybrid fibroblast-smooth muscle cell-like phenotype.

In summary, in this 2-D gel proteomic approach, we compared two methods of protein visualization and quantification. The modified protocol for metabolic labeling with [^{35}S]methionine showed a marked 3-fold improvement in the overall number of high-quality proteins spots detected and provided a more comprehensive study of the protein changes accompanying TGF-β_1 stimulation of human lung fibroblast. The results show that TGF-β_1 induces a whole set of actin-associated proteins involved in both actin polymerization and stabilization. These proteins accompany the induced expression of α-SMA and participate in the formation of stress fiber, cell contractility, and cell spreading characterizing the myofibroblasts phenotype.

* The costs of publication of this article were defrayed in part by the payment of page charges. This article must therefore be hereby marked "*advertisement*" in accordance with 18 U.S.C. Section 1734 solely to indicate this fact.

§ Current address: Active Biotech, AB Box 724, 220 07 Lund, Sweden.

‡‡ To whom correspondence should be addressed: AstraZeneca R&D Lund, Scheelevägen 8, SE-221 87 Lund, Sweden. Tel.: 46-46-336887; Fax: 46-46-337164; E-mail: gyorgy.marko-varga.@astrazeneca.com.

REFERENCES

1. Roche, W. R., Beasley, R., Williams, J. H., and Holgate, S. T. (1989) Subepithelial fibrosis in the bronchi of asthmatics. *Lancet* **1,** 520–524
2. Brewster, C. E., Howarth, P. H., Djukanovic, R., Wilson, J., Holgate, S. T., and Roche, W. R. (1990) Myofibroblasts and subepithelial fibrosis in bronchial asthma. *Am. J. Respir. Cell Mol. Biol.* **3,** 507–511
3. Gabbiani, G., Ryan, G. B., and Majne, G. (1971) Presence of modified fibroblasts in granulation tissue and their possible role in wound contraction. *Experientia* **27,** 549–550
4. Hebda, P. A., Collins, M. A., and Tharp, M. D. (1993) Mast cell and myofibroblast in wound healing. *Dermatol. Clin.* **11,** 685–696
5. Joyce, N. C., Haire, M. F., and Palade, G. E. (1987) Morphologic and biochemical evidence for a contractile cell network within the rat intestinal mucosa. *Gastroenterology* **92,** 68–81
6. Serini, G., and Gabbiani, G. (1999) Mechanisms of myofibroblast activity and phenotypic modulation. *Exp. Cell Res.* **250,** 273–283
7. Powell, D. W., Mifflin, R. C., Valentich, J. D., Crowe, S. E., Saada, J. I., and West, A. B. (1999) Myofibroblasts. I. Paracrine cells important in health and disease. *Am. J. Physiol.* **277,** C1–9
8. D'Amore, P. A. (1992) Capillary growth: A two-cell system. *Semin. Cancer Biol.* **3,** 49–56
9. Saunders, K. B., and D'Amore, P. A. (1992) An in vitro model for cell-cell interactions. *In Vitro Cell. Dev. Biol.* **28A,** 521–528
10. Villaschi, S., and Nicosia, R. F. (1994) Paracrine interactions between fibroblasts and endothelial cells in a serum-free coculture model. Modulation of angiogenesis and collagen gel contraction. *Lab. Invest.* **71,** 291–299
11. Tomasek, J. J., Gabbiani, G., Hinz, B., Chaponnier, C., and Brown, R. A. (2002) Myofibroblasts and mechano-regulation of connective tissue remodelling. *Nat. Rev. Mol. Cell. Biol.* **3,** 349–363
12. Fuchs, E., and Cleveland, D. W. (1998) A structural scaffolding of intermediate filaments in health and disease. *Science* **279,** 514–519
13. Iwasaki, H., Isayama, T., Ichiki, T., and Kikuchi, M. (1987) Intermediate filaments of myofibroblasts. Immunochemical and immunocytochemical analyses. *Pathol. Res. Practice* **182,** 248–254
14. Schmitt-Graff, A., Desmouliere, A., and Gabbiani, G. (1994) Heterogeneity of myofibroblast phenotypic features: An example of fibroblastic cell plasticity. *Virchows Arch.* **425,** 3–24
15. Torihashi, S., Gerthoffer, W. T., Kobayashi, S., and Sanders, K. M. (1994) Identification and classification of interstitial cells in the canine proximal colon by ultrastructure and immunocytochemistry. *Histochemistry* **101,** 169–183
16. Birchmeier, C., and Birchmeier, W. (1993) Molecular aspects of mesenchymal-epithelial interactions. *Annu. Rev. Cell Biol.* **9,** 511–540
17. Simon-Assmann, P., Kedinger, M., De Arcangelis, A., Rousseau, V., and Simo, P. (1995) Extracellular matrix components in intestinal development. *Experientia* **51,** 883–900
18. Apte, M. V., Haber, P. S., Applegate, T. L., Norton, I. D., McCaughan, G. W., Korsten, M. A., Pirola, R. C., and Wilson, J. S. (1998) Periacinar stellate shaped cells in rat pancreas: Identification, isolation, and culture. *Gut* **43,** 128–133
19. Border, W. A., and Noble, N. A. (1994) Transforming growth factor β in tissue fibrosis. *N. Engl. J. Med.* **331,** 1286–1292
20. Friedman, S. L. (1997) Closing in on the signals of hepatic fibrosis. *Gastro-*

enterology **112,** 1406–1409
21. Gressner, A. M. (1996) Transdifferentiation of hepatic stellate cells (Ito cells) to myofibroblasts: A key event in hepatic fibrogenesis. *Kidney Int.* **54,** (suppl.) S39–45
22. Kovacs, E. J., and DiPietro, L. A. (1994) Fibrogenic cytokines and connective tissue production. *FASEB J.* **8,** 854–861
23. Marra, F., Gentilini, A., Pinzani, M., Choudhury, G. G., Parola, M., Herbst, H., Dianzani, M. U., Laffi, G., Abboud, H. E., and Gentilini, P. (1997) Phosphatidylinositol 3-kinase is required for platelet-derived growth factor's actions on hepatic stellate cells. *Gastroenterology* **112,** 1297–1306
24. Zhang, K., Rekhter, M. D., Gordon, D., and Phan, S. H. (1994) Myofibroblasts and their role in lung collagen gene expression during pulmonary fibrosis. A combined immunohistochemical and in situ hybridization study. *Am. J. Pathol.* **145,** 114–125
25. Desmouliere, A., Geinoz, A., Gabbiani, F., and Gabbiani, G. (1993) Transforming growth factor-β1 induces α-smooth muscle actin expression in granulation tissue myofibroblasts and in quiescent and growing cultured fibroblasts. *J. Cell Biol.* **122,** 103–111
26. Ronnov-Jessen, L., and Petersen, O. W. (1993) Induction of alpha-smooth muscle actin by transforming growth factor-β1 in quiescent human breast gland fibroblasts. Implications for myofibroblast generation in breast neoplasia. *Lab. Invest.* **68,** 696–707
27. Sporn, M. B., and Roberts, A. B. (1992) Transforming growth factor-β: Recent progress and new challenges. *J. Cell Biol.* **119,** 1017–1021
28. Clouthier, D. E., Comerford, S. A., and Hammer, R. E. (1997) Hepatic fibrosis, glomerulosclerosis, and a lipodystrophy-like syndrome in PEPCK-TGF-β1 transgenic mice. *J. Clin. Invest.* **100,** 2697–2713
29. Hautmann, M. B., Madsen, C. S., and Owens, G. K. (1997) A transforming growth factor β (TGFβ) control element drives TGFβ-induced stimulation of smooth muscle α-actin gene expression in concert with two CArG elements. *J. Biol. Chem.* **272,** 10948–10956
30. Masur, S. K., Dewal, H. S., Dinh, T. T., Erenburg, I., and Petridou, S. (1996) Myofibroblasts differentiate from fibroblasts when plated at low density. *Proc. Natl. Acad. Sci. U. S. A.* **93,** 4219–4223
31. Muchaneta-Kubara, E. C., and el Nahas, A. M. (1997) Myofibroblast phenotypes expression in experimental renal scarring. *Nephrol. Dialysis Transplant.* **12,** 904–915
32. Shi, Y., O'Brien, J. E., Jr., Fard, A., and Zalewski, A. (1996) Transforming growth factor-β1 expression and myofibroblast formation during arterial repair. *Arterioscler. Thromb. Vasc. Biol.* **16,** 1298–1305
33. Tamm, E. R., Siegner, A., Baur, A., and Lutjen-Drecoll, E. (1996) Transforming growth factor-β1 induces α-smooth muscle-actin expression in cultured human and monkey trabecular meshwork. *Exp. Eye Res.* **62,** 389–397
34. Border, W. A., and Ruoslahti, E. (1992) Transforming growth factor-β in disease: The dark side of tissue repair. *J. Clin. Invest.* **90,** 1–7
35. Martin, P. (1997) Wound healing—Aiming for perfect skin regeneration. *Science* **276,** 75–81
36. Edlund, S., Landstrom, M., Heldin, C. H., and Aspenstrom, P. (2002) Transforming growth factor-β-induced mobilization of actin cytoskeleton requires signaling by small GTPases Cdc42 and RhoA. *Mol. Biol. Cell* **13,** 902–914
37. Bhowmick, N. A., Ghiassi, M., Bakin, A., Aakre, M., Lundquist, C. A., Engel, M. E., Arteaga, C. L., and Moses, H. L. (2001) Transforming growth factor-β1 mediates epithelial to mesenchymal transdifferentiation through a RhoA-dependent mechanism. *Mol. Biol. Cell* **12,** 27–36
38. Dugina, V., Alexandrova, A., Chaponnier, C., Vasiliev, J., and Gabbiani, G. (1998) Rat fibroblasts cultured from various organs exhibit differences in α-smooth muscle actin expression, cytoskeletal pattern, and adhesive structure organization. *Exp. Cell Res.* **238,** 481–490
39. Malmstrom, J., Westergren-Thorsson, G., and Marko-Varga, G. (2001) A proteomic approach to mimic fibrosis disease evolvement by an in vitro cell line. *Electrophoresis* **22,** 1776–1784
40. Baekkeskov, S., Warnock, G., Christie, M., Rajotte, R. V., Larsen, P. M., and Fey, S. (1989) Revelation of specificity of 64K autoantibodies in IDDM serums by high-resolution 2-D gel electrophoresis. Unambiguous identification of 64K target antigen. *Diabetes* **38,** 1133–1141
41. Shevchenko, A., Wilm, M., Vorm, O., and Mann, M. (1996) Mass spectrometric sequencing of proteins silver-stained polyacrylamide gels. *Anal. Chem.* **68,** 850–858
42. Gobom, J., Nordhoff, E., Mirgorodskaya, E., Ekman, R., and Roepstorff, P. (1999) Sample purification and preparation technique based on nanoscale reversed-phase columns for the sensitive analysis of complex peptide mixtures by matrix-assisted laser desorption/ionization mass spectrometry. *J. Mass Spectrom.* **34,** 105–116
43. Kawaguchi, T., Takeyasu, A., Matsunobu, K., Uda, T., Ishizawa, M., Suzuki, K., Nishiura, T., Ishikawa, M., and Taniguchi, N. (1990) Stimulation of Mn-superoxide dismutase expression by tumor necrosis factor-α: Quantitative determination of Mn-SOD protein levels in TNF-resistant and sensitive cells by ELISA. *Biochem. Biophys. Res. Commun.* **171,** 1378–1386
44. Byrjalsen, I., Mose Larsen, P., Fey, S. J., Nilas, L., Larsen, M. R., and Christiansen, C. (1999) Two-dimensional gel analysis of human endometrial proteins: Characterization of proteins with increased expression in hyperplasia and adenocarcinoma. *Mol. Hum. Reprod.* **5,** 748–756
45. Fey, S. J., and Larsen, P. M. (2001) 2D or not 2D. Two-dimensional gel electrophoresis. *Curr. Opin. Chem. Biol.* **5,** 26–33
46. Franzen, B., Auer, G., Alaiya, A. A., Eriksson, E., Uryu, K., Hirano, T., Okuzawa, K., Kato, H., and Linder, S. (1996) Assessment of homogeneity in polypeptide expression in breast carcinomas shows widely variable expression in highly malignant tumors. *Int. J. Cancer* **69,** 408–414
47. Zhang, H. Y., Gharaee Kermani, M., Zhang, K., Karmiol, S., and Phan, S. H. (1996) Lung fibroblast α-smooth muscle actin expression and contractile phenotype in bleomycin-induced pulmonary fibrosis. *Am. J. Pathol.* **148,** 527–537
48. Kanamoto, T., Hellman, U., Heldin, C. H., and Souchelnytskyi, S. (2002) Functional proteomics of transforming growth factor-β1-stimulated Mv1Lu epithelial cells: Rad51 as a target of TGFβ1-dependent regulation of DNA repair. *EMBO J.* **21,** 1219–1230
49. Wrana, J. L., Overall, C. M., Sodek, J. (1991) Regulation of the expression of a secreted acidic protein rich in cysteine (SPARC) in human fibroblasts by transforming growth factor β. Comparison of transcriptional and post-transcriptional control with fibronectin and type I collagen. *Eur. J. Biochem.* **197,** 519–528
50. Skonier, J., Neubauer, M., Madisen, L., Bennett, K., Plowman, G. D., and Purchio, A. F. (1992) cDNA cloning and sequence analysis of beta ig-h3, a novel gene induced in a human adenocarcinoma cell line after treatment with transforming growth factor-β. *DNA Cell Biol.* **11,** 511–522
51. Hatakeyama, D., Kozawa, O., Niwa, M., Matsuno, H., Ito, H., Kato, K., Tatematsu, N., Shibata, T., and Uematsu, T. (2002) Upregulation by retinoic acid of transforming growth factor-β-stimulated heat shock protein 27 induction in osteoblasts: Involvement of mitogen-activated protein kinases. *Biochim. Biophys. Acta* **1589,** 15–30
52. Hautmann, M. B., Adam, P. J., and Owens, G. K. (1999) Similarities and differences in smooth muscle α-actin induction by TGF-β in smooth muscle versus non-smooth muscle cells. *Arterioscler. Thromb. Vasc. Biol.* **19,** 2049–2058
53. Ueki, N., Ohkawa, T., Yamamura, H., Takahashi, K., Tsutsui, T., Kawai, Y., Yokoyama, Y., Amuro, Y., Hada, T., and Higashino, K. (1998) Induction of calponin-h1 by transforming growth factor-β1 in cultured human ito cells, LI90. *Biochim. Biophys. Acta* **1403,** 28–36
54. Bamburg, J. R., McGough, A., and Ono, S. (1999) Putting a new twist on actin: ADF/cofilins modulate actin dynamics. *Trends Cell Biol.* **9,** 364–370
55. Pollard, T. D., and Borisy, G. G. (2003) Cellular motility driven by assembly and disassembly of actin filaments. *Cell* **112,** 453–465
56. Zebda, N., Bernard, O., Bailly, M., Welti, S., Lawrence, D. S., and Condeelis, J. S. (2000) Phosphorylation of ADF/cofilin abolishes EGF-induced actin nucleation at the leading edge and subsequent lamellipod extension. *J. Cell Biol.* **151,** 1119–1128
57. Abe, H., Ohshima, S., and Obinata, T. (1989) A cofilin-like protein is involved in the regulation of actin assembly in developing skeletal muscle. *J. Biochem.* **106,** 696–702
58. Ichetovkin, I., Grant, W., and Condeelis, J. (2002) Cofilin produces newly polymerized actin filaments that are preferred for dendritic nucleation by the Arp2/3 complex. *Curr. Biol.* **12,** 79–84
59. Blanchoin, L., Pollard, T. D., and Hitchcock-DeGregori, S. E. (2001) Inhibition of the Arp2/3 complex-nucleated actin polymerization and branch formation by tropomyosin. *Curr. Biol.* **11,** 1300–1304
60. Nishida, E., Muneyuki, E., Maekawa, S., Ohta, Y., and Sakai, H. (1985) An actin-depolymerizing protein (destrin) from porcine kidney. Its action on F-actin containing or lacking tropomyosin. *Biochemistry* **24,** 6624–6630
61. Bernstein, B. W., and Bamburg, J. R. (1982) Tropomyosin binding to F-actin

protects the F-actin from disassembly by brain actin-depolymerizing factor (ADF). *Cell Motil.* **2,** 1–8
62. Ono, S., and Ono, K. (2002) Tropomyosin inhibits ADF/cofilin-dependent actin filament dynamics. *J. Cell Biol.* **156,** 1065–1076
63. DesMarais, V., Ichetovkin, I., Condeelis, J., and Hitchcock-DeGregori, S. E. (2002) Spatial regulation of actin dynamics: A tropomyosin-free, actin-rich compartment at the leading edge. *J. Cell Sci.* **115,** 4649–4660
64. King-Briggs, K. E., and Shanahan, C. M. (2000) TGF-β superfamily members do not promote smooth muscle-specific alternative splicing, a late marker of vascular smooth muscle cell differentiation. *Differentiation* **66,** 43–48
65. Nagumo, H., Seto, M., Sakurada, K., Walsh, M. P., and Sasaki, Y. (1998) HA1077, a protein kinase inhibitor, inhibits calponin phosphorylation on Ser175 in porcine coronary artery. *Eur. J. Pharmacol.* **360,** 257–264
66. Kaneko, T., Amano, M., Maeda, A., Goto, H., Takahashi, K., Ito, M., and Kaibuchi, K. (2000) Identification of calponin as a novel substrate of Rho-kinase. *Biochem. Biophys. Res. Commun.* **273,** 110–116
67. Mann, M., Ong, S. E., Gronborg, M., Steen, H., Jensen, O. N., and Pandey, A. (2002) Analysis of protein phosphorylation using mass spectrometry: Deciphering the phosphoproteome. *Trends Biotechnol.* **20,** 261–268
68. Deloulme, J. C., Assard, N., Mbele, G. O., Mangin, C., Kuwano, R., and Baudier, J. (2000) S100A6 and S100A11 are specific targets of the calcium- and zinc-binding S100B protein *in vivo. J. Biol. Chem.* **275,** 35302–35310
69. Arcuri, C., Giambanco, I., Bianchi, R., and Donato, R. (2002) Subcellular localization of S100A11 (S100C, calgizzarin) in developing and adult avian skeletal muscles. *Biochim. Biophys. Acta* **1600,** 84–94
70. Sakaguchi, M., Miyazaki, M., Kondo, T., and Namba, M. (2001) Up-regulation of S100C in normal human fibroblasts in the process of aging in vitro. *Exp. Gerontol.* **36,** 1317–1325
71. Sakaguchi, M., Miyazaki, M., Inoue, Y., Tsuji, T., Kouchi, H., Tanaka, T., Yamada, H., and Namba, M. (2000) Relationship between contact inhibition and intranuclear S100C of normal human fibroblasts. *J. Cell Biol.* **149,** 1193–1206
72. Sakaguchi, M., Tsuji, T., Inoue, Y., Miyazaki, M., Namba, M., Yamada, H., and Tanaka, T. (2001) Loss of nuclear localization of the S100C protein in immortalized human fibroblasts. *Radiat. Res.* **155,** 208–214